Control of Enhanced Virtual Synchronous Generator For Parallel Inverters In Microgrids

G.Venkatesh [1], S.Venkat Rao [2]
[1]Dept of EEE
[2]Assistant professor, Dept of EEE
[1, 2] SVPCET PUTTUR.

Abstract- *Virtual synchronous generator (VSG) control is a promising communication-less control method in a microgrid for its inertia support feature. However, active power oscillation and improper transient active power sharing are observed when basic VSG control is applied. Moreover, the problem of reactive power sharing error, inherited from conventional droop control, should also be addressed to obtain desirable stable state per-formance. In this paper, an enhanced VSG control is proposed, with which oscillation damping and proper transient active power sharing are achieved by adjusting the virtual stator reactance based on state-space analyses. Furthermore, communication-less accurate reactive power sharing is achieved based on inversed voltage droop control feature (V–Q droop control) and common ac bus voltage estimation. Simulation and experimental results verify the improvement introduced by the proposed enhanced VSG control strategy.*

Keywords- DC-AC power converters, distributed power generation, droop control, microgrids, power control, power sys-tem dynamics, power system modeling, reactive power control, state-space methods, virtual synchronous generator.

I. INTRODUCTION

RECENT years, inverter-interfaced distributed generator (DGs) with renewable energy sources (RES), e.g., photovoltaics and wind turbines, have been developed to solve energy crisis and environmental issues. To facilitate the inte-gration of DGs in distribution system, the concept of microgrid is proposed . The control strategies of microgrids are pre-ferred to be in a communication-less manner because of its decentralized feature. Although in a hierarchical microgrid control structure, communication is required for the secondary and tertiary control, it is still recommended to realize the basic functions of a microgrid in the primary control level with-out communication . Droop control is a widely adopted communication-less control method in a microgrid. By droop-ing the frequency against the active power (P–ω droop) and the output voltage against reactive power (Q–V droop), load shar-ing between DGs can be performed in an autonomic manner, which is similar to the power sharing between parallel syn-chronous generators (SGs) . In some references , it is proposed that P–V and Q–ω droop controls are more suit-able for low voltage (LV) microgrid in the light of the resistive line impedance feature. Meanwhile, the P–ω and Q–V droop controls are still valid in LV microgrid by adding inductive virtual impedance .

However, like most of DG control methods, a conven-tional droop control provides barely any inertia support for the microgrid, thus a droop-control-based microgrid is usually inertia-less and sensitive to fault. To provide inertia support for the system, control methods to emulate virtual inertia are proposed in recent literatures, such as virtual synchronous generator (VSG), virtual synchronous machine and synchronverter . Although their name and con-trol scheme differ from each other, the principles are similar in the aspect that all of them mimic the transient characteristics of SG by emulating its fundamental swing equation. For sim-pler explication, all of these methods are called VSG control in this paper. A comprehensive survey on VSGs and the exist-ing topologies are given in . Besides, a unique method to provide virtual inertia by modifying the droop coefficient in droop control is presented in . To share the load in parallel operation, droop characteristics are also emulated in some VSG control schemes . In this case, as it is demonstrated in and , VSG control inherits the advantages of droop control, and outperforms the latter in terms of transient frequency stability owing to its lower df /dt rate. Therefore, VSG control can be considered as a poten-tial upgrade for the communication-less control method of a microgrid.

However, when VSG control is applied in microgrids, several problems have been noticed, such as oscillation in active power during a disturbance, inappropriate transient active power sharing during loading transition and errors in reactive power sharing.

Active power oscillation during a disturbance is introduced by the well-known feature of the swing equation, thus it is an inherent feature for a real SG as well as a VSG. It is not a critical problem for SGs because they usually have considerable overload capabilities, but the overload capabil-

ities of inverter-interfaced DGs are not high enough to ride though a large oscillation. However, this oscillation can be damped by properly increasing the damping ratio or using alternating moment of inertia . Using smaller iner-tia may also lead to reduced oscillation however, it is not encouraged because providing a large amount of virtual iner-tia is an advantage that distinguishes VSG from other control methods.

In this paper, a novel method for oscillation damping is proposed based on increasing the virtual stator reactance. Due to the oscillatory feature of VSG, inappropriate tran-sient active power sharing during loading transition may also cause oscillation, which is avoidable if the swing equa-tion and output impedance are designed properly, as it is analyzed in this paper. Sharing transient loads between SG and DG is addressed in , but theoretical analysis is not provided.

The inaccurate reactive power sharing is a well-known problem in conventional *Q*–*V* droop control, and the same problem is reported in active power sharing of *P*–*V* droop control. In *Q*–*V* or *P*–*V* droop controls, output voltage is regu-lated according to reactive/active power sharing, but the output voltage of each DG is not equal due to unequal line voltage drop. This problem has received considerable attention in the literature, and many control strategies are proposed to address this issue . A comprehensive solution is to eliminate the mismatch of DG output impedance however, this method cannot guarantee accurate reactive power sharing if active power is not shared according to the power rating ratio. An approach based on line voltage drop compensation is proposed in . However, a grid-connected mode operation is required for the evaluation of line parameters, which is not feasible for an isolated microgrid. Other communication-less approaches, e.g., Q–dV/ dt droop control , adaptive voltage droop, and virtual capacitor control are also proposed. However, the reactive power sharing errors cannot be completely eliminated by these methods, as it is demonstrated in respective experimental results. In some approaches, communication is used to improve reactive power sharing accuracy, such as secondary control signals from MGCC , master-slave communication , and communication between DGs . However, as accurate reactive power sharing is a basic function of a microgrid, it is always preferred to solve this problem in a communication-less manner considering the probable communication fault.

In this paper, a communication-less approach is proposed based on inversed voltage droop control (*V*–*Q* droop con-trol) and common ac bus voltage estimation. By applying the proposed method, reactive power sharing is immune to line impedance mismatch and active power sharing change. The idea to use ac bus voltage as a common refer-ence shares some similarities with the approaches presented in and . However, in these works, measured bus voltage is used directly; while, in microgrid appli-cations, it may not be feasible if DGs are not installed in the proximity of the ac bus. In this paper, bus volt-age is estimated based on the available local measurement, thus there should be no installation difficulty in the field applications.

The rest of this paper is organized as follows. In Section II, a brief description of the basic VSG control is presented. In Section III, a state-space model of islanded microgrid using VSG control is built, and the principle of proposed oscillation damping method is derived from eigenvalue analysis of this model. Proper parameter design for appropriate transient load sharing based on poles-zeros cancellation is also discussed based on the same model. In Section IV, the cause of reactive power sharing errors is discussed and a novel accurate reactive power sharing method is proposed. The enhanced VSG control strategy is presented in Section V. Simulation and experiment results are shown in Sections VI and VII, respectively. Finally, conclusions are given in Section VIII.

II. BASIC VSG CONTROL SCHEME

Fig. 1 shows the structure of a DG using the basic VSG control . The primary source of the DG could be photovoltaic panels, fuel cells, a gas engine or other distributed energy resources (DERs). The energy storage is designed for emulating the kinetic energy stored in rotating mass of a SG, in order to supply or absorb insufficient/surplus power generated by the primary source in transient state . As this paper focuses on the control scheme of the inverter, the design and

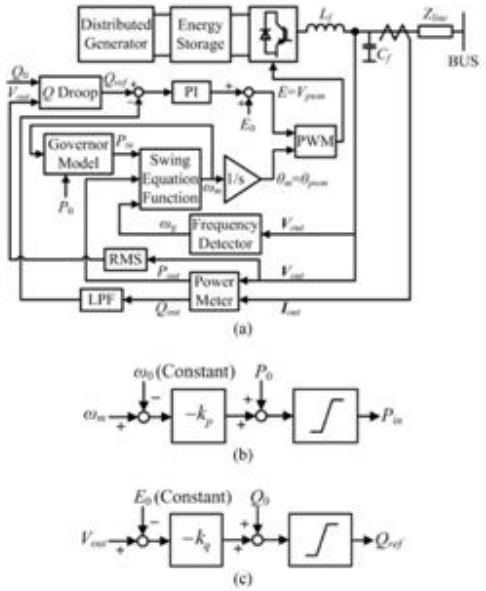

Fig. 1. Block diagram of (a) the basic VSG control, (b) the "Governor Model" block and (c) the "*Q* Droop" block.

control of the primary source and energy storage are beyond the scope of this paper.

In the block "Swing Equation Function" in Fig. 1(a), ω_m is solved from the swing equation (1) by an iterative method.

$$P_{in} - P_{out} = J\omega_m \frac{d\omega_m}{dt} + D(\omega_m - \omega_g) \quad (1)$$

The block "Governor Model" in Fig. 1(a) is a ω–P droop controller as shown in Fig. 1(b). In some previous studies , a first order lag unit is used to emulate the mechanical delay in the governor of a real SG. However, in this paper, this delay is removed, because it degrades the dynamic performance of DG, as it is discussed in .

The block "*Q* Droop" in Fig. 1(a) is a *V*–*Q* droop controller as shown in Fig. 1(c), which differs from the conventional *Q*–*V* droop controller in the reversed input and output. It is noteworthy that inner current or voltage loop is not adopted in this control scheme, in order to make the filter induc-tor L_f contribute to the output impedance and be considered as the stator inductance of the VSG. This stator inductance results in more inductive output impedance, which is espe-cially important for active and reactive power decoupling in a low voltage microgrid in which line resistance is dominant. Nevertheless, output voltage is still regulated indirectly by the *V*–*Q* droop controller and the PI controller of reactive power. In order to diminish the influence from ripples in measured output power, a 20Hz 1st order low-pass filter is applied for Q_{out} as shown in Fig. 1(a). As the output current is mea-sured after the LC filter stage, the reactive power consumed

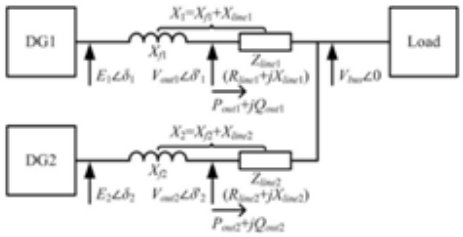

Fig. 2. Structure of a microgrid in islanded mode.

by the LC filter is not included in Q_{out}. Therefore, no spe-cific inertial process is required for the reactive power PI controller.

In a microgrid, in order to share the active and reactive power according to the ratings of DGs without communication,

$k_p^* = (k_p\omega_0)/S_{base}$, $k_q^* = (k_qE_0)/S_{base}$, $P^*_0 = P_0/S_{base}$ and $Q^*_0 = Q_0/S_{base}$ should be designed equally for each DG in default . In this paper, to simplify the explication for the case of different power ratings, per unit values are calculated based on respective power ratings of DGs.

III. ANALYSES OF TRANSIENT ACTIVE POWER PERFORMANCE

A. Closed-Loop State-Space Model

In the present work, an islanded microgrid which consists of two DGs using VSG control is studied, as it is shown in Fig. 2. The DGs are connected to a common ac bus via a distri-bution line, to supply the loads in the microgrid. Note that the capacitor of the DG output LC filter in Fig. 1 is neglected, as its susceptance is usually negligible at fundamental frequency.

In order to understand the reasons of active power oscil-lation and to find proper solutions, a state-space model for the closed-loop active power control of the microgrid shown in Fig. 2 can be obtained as given in , of which the deduction process is shown in . To simplify the model and focus on the specific eigenvalues causing oscillation, the reactive power part is not included in this model and the line resistance is neglected in inductive output impedance point of view. It is shown in that these simplifications do not affect the precision of the model.

$$\dot{x} = Ax + Bw \quad (2)$$
$$y = Cx + Dw$$

where

$$w = \begin{bmatrix} P_{load} & P_{0\_1} & P_{0\_2} & T \end{bmatrix} \quad (3)$$
$$y = \begin{bmatrix} \omega_{m1} & \omega_{m2} & P_{out1} & P_{out2} & T \end{bmatrix} \quad (4)$$
$$x = \begin{bmatrix} \omega_{m1} + \frac{D_1}{J_1\omega_0(K_1+K_2)} P_{load} \\ \omega_{m2} + \frac{D_2}{J_2\omega_0(K_1+K_2)} P_{load} \\ \delta_1 - \frac{K_1}{K_1+K_2} P_{load} \end{bmatrix} \quad (5)$$

□

and $\boldsymbol{A}$ and $\boldsymbol{B}$ are shown in (6) and (7), respectively, at the bottom of the page. Here, $K_i = (E_i V_{bus}\cos\delta_i)/X_i$, and $X_i \approx {}^{X}f\,i + {}^{X}line\,i$

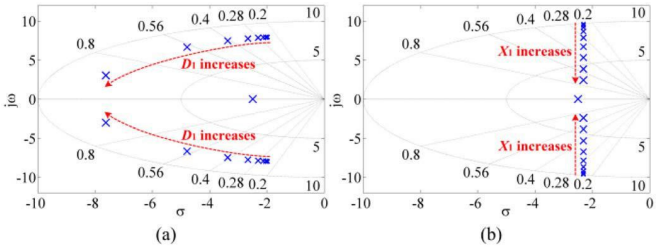

Fig. 3. Eigenvalue loci with a variation of (a) D^*_1 ($2^{-4} \times 17$ pu ~ $2^5 \times 17$ pu) or (b)

TABLE I
STATE-SPACE MODEL PARAMETERS

Parameter	Value	Parameter	Value
S_{base1}	10 kVA	M_i^*	8 s
S_{base2}	5 kVA	D_i^*	17 pu
E_0	200 V	$k_{p\,i}^*$	20 pu
ω_0	376.99 rad/s	X_i^*	0.7 pu
$E_i = V_{bus}$	200 V		

Analyses of transient active power control performance in the following parts of present section are based on this model, as it describes the transient performance of variables in $\boldsymbol{y}$ after a given disturbance $\boldsymbol{w}$.

B. Oscillation Damping

It is a known conclusion in the control theory that the poles of transfer function of $Y_j(s)/W_k(s)$ are available in the eigenvalues of $\boldsymbol{A}$, for any j, k. Therefore, the studies on eigenvalues of $\boldsymbol{A}$ should give some clues to damping methods for oscillations in $P_{out\,i}$.

The loci of eigenvalues of $\boldsymbol{A}$ with a variation of D_1 or X_1 are shown in Fig. 3. Nominal parameters are listed in Table I,

in which $M_i^* = (J_i\omega_0^2)/S_{base\ i}$, $D^*_i = (D_i\omega_0)/S_{base\ i}$, and $X_i^* = (X_i S_{base\,i})/E_0^2$.

In the eigenvalue loci plots, radial dash lines indicate damping ratio ζ, and circle dash lines indicate natural frequency ω_n. As it is shown in Fig. 3, damping ratio of the complex-conjugate eigenvalues increases if the damping fac-tor D_i and/or the output reactance impedance X_i are increased. It should be pointed out that increasing X_i causes a decrease in damped natural frequency ω_d, which is indicated by the distance between eigenvalue and the real axis. This may result in longer settling time compared to the method of increas-ing D_i. However, the approach of increasing output reactance has other merits as follows.

1) The state-space model is obtained under the assumption that the output impedance of DGs is inductive.

This assumption is less valid if X_i is small, especially in a LV microgrid in which the line impedances are mainly resistive. If this assumption is not valid, the active power and reactive power control cannot be decoupled correctly and the system may become more oscillatory and even unstable.

2) To share transient active power properly, output reac-tance of each DG should be designed equally in per unit value, as it is discussed in the next part of this section. Therefore, the problem of oscillation and that of tran-sient active power sharing can be solved simultaneously by proper stator reactance design.

3) Moreover, the influence of output reactance mismatch on transient active power sharing becomes smaller if output reactance of DGs is increased, owing to decreased relative errors.

$$\begin{bmatrix} -\frac{D_1K_2}{J_1\omega_0(K_1+K_2)} - \frac{k_{p1}}{J_1\omega_0} & \frac{D_1K_2}{J_1\omega_0(K_1+K_2)} & \frac{K_1}{J_1\omega_0} \\ \frac{D_2K_1}{J_2\omega_0(K_1+K_2)} & -\frac{D_2K_1}{J_2\omega_0(K_1+K_2)} - \frac{k_{p2}}{J_2\omega_0} & -\frac{K_2}{J_2\omega_0} \\ \frac{K_2}{K_1+K_2} & -\frac{K_2}{K_1+K_2} & 0 \end{bmatrix}$$

$$\begin{bmatrix} -\frac{K_1}{J_1\omega_0(K_1+K_2)} - \frac{D_1D_2K_1}{J_1J_2\omega_0^2(K_1+K_2)^2} + \frac{D_1^2K_2}{J_1^2\omega_0^2(K_1+K_2)^2} + \frac{D_1k_{p1}}{J_1^2\omega_0^2(K_1+K_2)} \\ -\frac{1}{J_2\omega_0} + \frac{K_1}{J_2\omega_0(K_1+K_2)} - \frac{D_1D_2K_1}{J_1J_2\omega_0^2(K_1+K_2)^2} + \frac{D_2^2K_1}{J_2^2\omega_0^2(K_1+K_2)^2} + \frac{D_2k_{p2}}{J_2^2\omega_0^2(K_1+K_2)} \\ \frac{K_2}{K_1+K_2} - \frac{K_2D_1}{J_1\omega_0(K_1+K_2)^2} + \frac{K_2D_2}{J_2\omega_0(K_1+K_2)^2} \end{bmatrix}$$

C. Transient Active Power Sharing

The response of output active power of DGs during a loading transition can be calculated from transfer func-tions

$P_{out1}(s)/\ P_{load}(s)$ and $P_{out2}(s)/\ P_{load}(s)$, which are the elements $G_{31}(s)$ and $G_{41}(s)$ of the matrix $\boldsymbol{G}(s)$ shown in (10), respectively.

$$\boldsymbol{G}(s) = \boldsymbol{C}(s\boldsymbol{I} - \boldsymbol{A})^{-1}\boldsymbol{B} + \boldsymbol{D}. \qquad (10)$$

The loci of poles and zeros of $P_{out1}(s)/\ P_{load}(s)$ and $P_{out2}(s)/\ P_{load}(s)$ are shown in Fig. 4. It is shown that if the per unit value of X_i^*, M_i^*, and D^*_i of each DG are set equally, all poles are cancelled by zeros. This cancellation implies a desirable step change of P_{out1} and P_{out2} directly to their respective steady-state values without any oscillation during a loading transition. Equal values of M_i^* and D^*_i are not difficult to realize since they are virtual parameters that can be easily changed in the VSG control program. As for X_i^*, a control method to adjust stator reactance is presented in Section V.

IV. IMPROVEMENT OF REACTIVE POWER SHARING

Fig. 5 shows the principles of ω–P and V–Q droop controls in the "Governor Model" and "Q Droop" blocks shown in Fig. 1 for the case of S_{base1}: S_{base2} = 2 : 1. As discussed in Section II, k_p^*, k_q^*, P^*_0 and Q^*_0 are designed equally. Based on the predefined linear droop characteristic, the desired power sharing P_{in1}: P_{in2} = 2 : 1 can be obtained because the governor input is ω_m, and $\omega_{m1} = \omega_{m2}$ is guaranteed in steady state.

Following the same principle, to share the reactive power according to the power rating ratio, an equal voltage reference is required. However, for the V–Q droop in basic VSG control shown in Fig. 1(c), the voltage reference is the inverter output voltage, which may be a different value for each DG even in steady state due to the line voltage drop. As most of previous studies are based on Q–V droop, in which the output voltage should be regulated based on measured reactive power

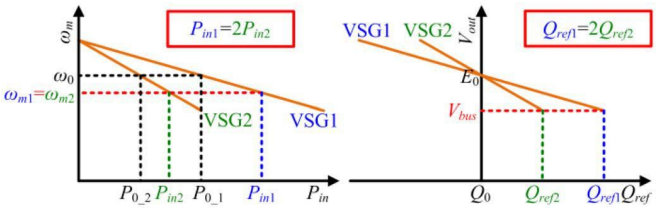

Fig. 5. Principles of ω–P and V–Q droop control.

by equalizing the output impedance, or to compensate the line voltage drop . Both methods need great effort in design process and complex computations in DG control law, whereas the resulted reactive power sharing is still influ-enced by active power sharing. As the voltage does not need to be controlled directly in a V–Q droop control scheme shown in Fig. 1(a), the reference voltage can be chosen other than inverter output voltage. If the common ac bus voltage V_{bus} is used instead of inverter output voltage $V_{out\ i}$, equal reactive power reference value $Q_{ref\ 1} = Q_{ref\ 2}$ can be guaranteed, as it is illustrated in Fig. 5. Therefore, accurate reactive power sharing $Q_{out1} = Q_{out2}$ should be obtained through the using of reactive power PI controller. Moreover, unlike output voltage, bus voltage is not influenced by line voltage drop, which is determined by both active and reactive power. Therefore, reac-tive power sharing according to the bus voltage is independent from active power.

In some previous researches direct bus voltage measurement is suggested. However, in the field appli-cations, it is difficult to measure V_{bus} directly, as DGs may be installed far away from the common ac bus, and the utilization of communication is not preferred for reliability reason. Therefore, a bus voltage estimation method using local measurement is proposed in next section.

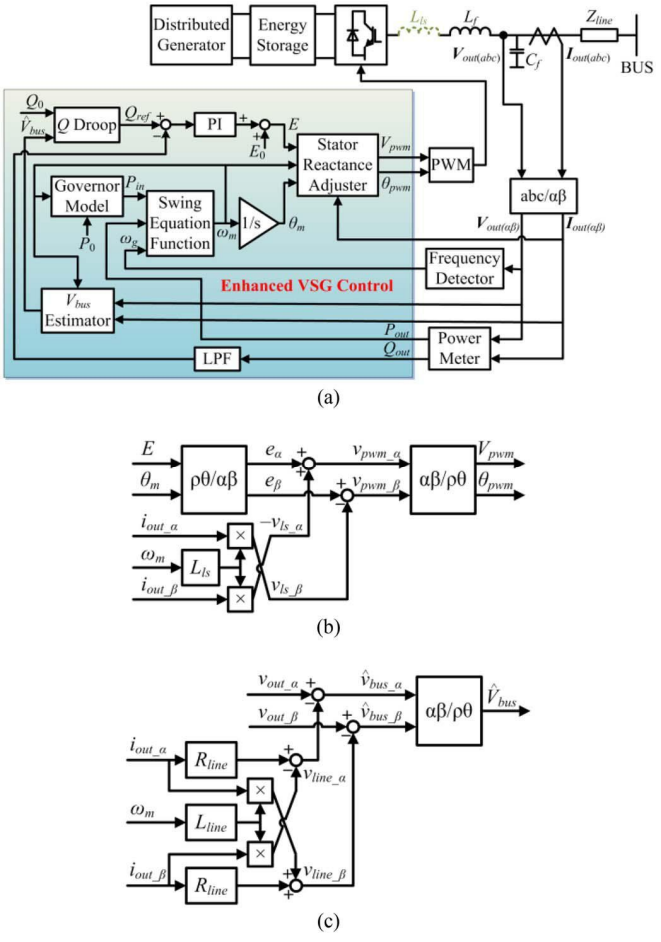

Fig. 6. Block diagram of (a) the proposed enhanced VSG control, (b) the "Stator Reactance Adjuster" block and (c) the "Vbus Estimator" block.

V. PROPOSED ENHANCED VSG CONTROL SCHEME

The proposed enhanced VSG control scheme is shown in Fig. 6. Compared to the basic VSG control, two major modifi-cations are made, i.e., the stator reactance adjuster and the bus voltage estimator, as shown in Figs. 6(b) and 6(c), respectively.

The function of stator reactance adjuster is to adjust the output reactance of the DG freely. It is operating as a virtual impedance controller. The virtual stator inductor is realized by multiplying output current by the virtual stator inductor in stationary frame. It will be more accuracy if inductor current through L_f is used. However, this increases the number of current sensors, which is not necessary. As the current flowing into C_f at fundamental frequency is less than few percent of the inductor current, using output current instead of inductor current does not affect the performance of the control scheme.

Based on the given analyses in Section III and according to (11), tuning of virtual stator inductor L_{ls} is suggested to set total output reactance X_i^* for both DGs in same large per unit value. This approach increases active power damping ratio and shares transient load without oscillation. The target value is proposed to be 0.7 pu because it is a typical value for the total direct-axis transient reactance X_d of a real SG.

$$X_i^* = S_{base\,i}\omega_{m\,i}(L_{ls\,i} + L_{f\,i} + L_{line\,i})/E_0^2 = 0.7 \text{ pu}.$$

The $L_{f\,i}$ and $Z_{line\,i}$ ($R_{line\,i} + jL_{line\,i}$) are considered as known parameters in this paper. As the scale of microgrid is usu-ally small, the line distance is easily to be measured or fed by the planner. Even if it is not the case, several online mea-surement or intelligent tuning methods for $Z_{line\,i}$ are available in [42] and [43].

With the proposed design of stator reactance adjustment, oscillation in a VSG-control-based microgrid should be almost eliminated during a loading transition in islanded mode. Particularly, transition from grid-connected mode to islanded mode can also be considered as a loading transition; therefore, the oscillation during an islanding event should also be elim-inated with the proposed control strategy, as it is proved by simulation results in next section. As for other disturbances in islanded mode, e.g., change of active power set value of DG(s), connection/disconnection of DG(s), etc., oscillation cannot be eliminated, but can still be damped by the increased total output reactance.

The principle of bus voltage estimator in Fig. 6(c) is sim-ilar to that of stator reactance adjuster in Fig. 6(b). By calculating the line voltage drop in stationary frame using measured output current and line impedance data, the bus voltage can be estimated from the difference of output volt-age and calculated line voltage drop. Since the RMS value of estimated bus voltage V_{bus} for each DG should be approx-imately equal, as it is discussed in last section, accurate reactive power sharing can be obtained by using estimated bus voltages as the input references of "Q Droop" instead of respective output voltages of DGs. Although the principle of presented bus voltage estimator is not new, the idea of using this estimator to realize communication-less accurate reac-tive power sharing can be considered as a contribution in the present work.

However, if there is an estimation error in V_{bus}, it will cause a reactive power sharing error. Supposing V^* and V^*

$$V^* \quad V^*, \qquad V^*_{bus1} = V^*_{bus} + \hat{}_1 \quad V^*_{bus2} = V^*_{bus} + \hat{}_2$$

$$Q^* \quad Q^* \qquad k^*(V^* \quad V^*). \qquad (12)$$

$$Q^*_{out1} - Q^*_{out2} = -k^*_q(\hat{}_1 - \hat{}_2)$$

That is to say, the reactive power sharing error caused by estimation errors is determined by the V–Q droop gain k_q^*. The design of k_q^* is a well-known trade-off between voltage deviation and reactive power control accuracy. Considering the probable ripples in the measured RMS value of V_{bus}, k_q is recommended to be 5 pu for the present example.

It should be pointed out that the increased output reactance by adding the virtual stator inductor L_{ls} causes a decrease in the reactive control plant gain, as shown in Fig. 7. Therefore, to obtain a same bandwidth of 20 Hz for the reactive power control loop, the gain of PI controller should be increased to compensate the decreased plant gain, as illustrated in Fig. 8. The parameters used to plot Fig. 8 are related to DG1, which are shown in Fig. 9 and Table II. The 20Hz bandwidth is relatively low compared to control methods working on instan-taneous value; however, it is fast enough to track the reactive power and regulate the output voltage as it is demonstrated in the simulation and experimental results.

VI. SIMULATION RESULTS

Simulations are executed in PSCAD/EMTDC environment to verify the effectiveness of the proposed enhanced VSG con-trol scheme. A microgrid shown in Fig. 9 is studied. As it is shown in Fig. 9, impedances of output

filters and lines of each DG differ in per unit values. Other main parameters are listed in Table II, and the sequence of simulation is shown in Table III. Events of islanding from grid, loading transition, and intentional active power sharing change are simulated at 21 s, 24 s, and 27 s, respectively. The simulation results are shown in Fig. 10.

As it is illustrated in Fig. 10(a), when the microgrid is islanded at 21 s, and when load 2 is connected at 24 s,

TABLE II
SIMULATION PARAMETERS

Common Parameters			
Parameter	Value	Parameter	Value
S_{base1}	10 kVA	M_i^*	8 s
S_{base2}	5 kVA	D_i^*	17 pu
$E_0 = V_{grid}$	200 V	$k_{p\,i}^*$	20 pu
$\omega_0 = \omega_{grid}$	376.99 rad/s	$k_{q\,i}^*$	5 pu
$P_{0\,i}^*$	1 pu	$T_{fq\,i}$	7.96×10^{-3} s
$Q_{0\,i}^*$	0 pu		
Basic VSG control			
$K_{pq\,i}^*$	0.0025 pu	$T_{lq\,i}$	1.25×10^{-4} s
Enhanced VSG control			
$K_{pq\,i}^*$	0.0125 pu	$T_{lq\,i}$	1.25×10^{-4} s

TABLE III
SIMULATION SEQUENCE

Time	Grid	$P_{0\,1}^*$	$P_{0\,2}^*$	Load
$t < 21$ s	Connected	1 pu	1 pu	Load1
21 s $\leq t <$ 24 s	Disconnected	–	–	–
24 s $\leq t <$ 27 s	–	–	–	Load1+2
27 s $\leq t <$ 30 s	–	–	0.6 pu	–

oscillation can be observed in active power when the basic VSG control is applied for both DGs. This oscillation is almost eliminated by applying the proposed enhanced VSG control shown in Fig. 10(b). As the disturbance at 27 s is caused by change of active power set value of DG1, which is not a loading transition, active power oscillation cannot be elim-inated in this case. However, the proposed enhanced VSG control increases the damping ratio; therefore, the overshoots in Fig. 10(b) are smaller than that in Fig. 10(a). Meanwhile, the oscillation periods become longer, because the damped natural frequencies are decreased as it is discussed in Section III-B. Note that the rate of change of frequency remains the same in all cases, which suggests that the proposed enhanced VSG control has no influence on the inertia support feature of VSG control.

Moreover, in the case of the basic VSG control, reactive power is not shared properly in islanded mode, and is not controlled at set value in grid-connected mode, due to the volt-age drop through the line impedance, as shown in Fig. 10(a). Besides, reactive power control is not independent from active power control, as a change of set value of active power at 27 s also causes a change of reactive power sharing. These prob-lems are all solved in the enhanced VSG control, as it is shown in Fig. 10(b). It is also noteworthy that the steady-state devi-ations of DG voltage and bus voltage become smaller when the enhanced VSG control is applied.

Fig. 11 illustrates the dynamic performance of reactive power and voltage during the loading transition at 24 s. Although the virtual internal emf E_1 becomes much higher in the proposed enhanced VSG control owing to the voltage drop on virtual stator inductance L_{ls}, the maximum voltage sag of PWM inverter reference V_{pwm1} and output voltage V_{out1} are kept within the same level as the basic VSG control. This implies that the voltage drop on L_{ls} is compensated well by the reactive power PI controller. Besides, although in the enhanced VSG control, the voltage becomes slightly oscillatory, the reactive power oscillation converges within 0.1 s.

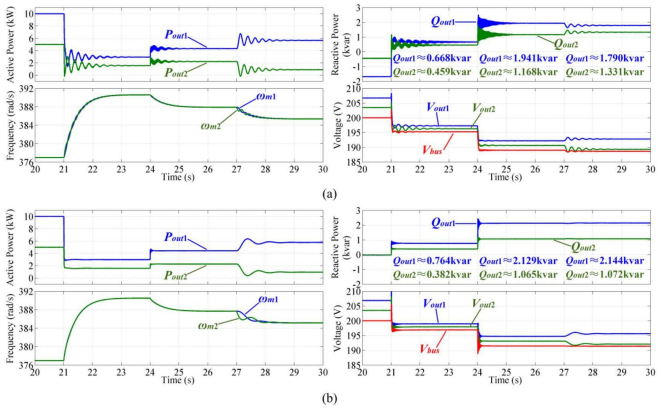

Fig. 10. Simulation results of active power and frequency in the left column and reactive power and voltage in the right column when both DGs are controlled by (a) the basic VSG control, (b) the proposed enhanced VSG control.

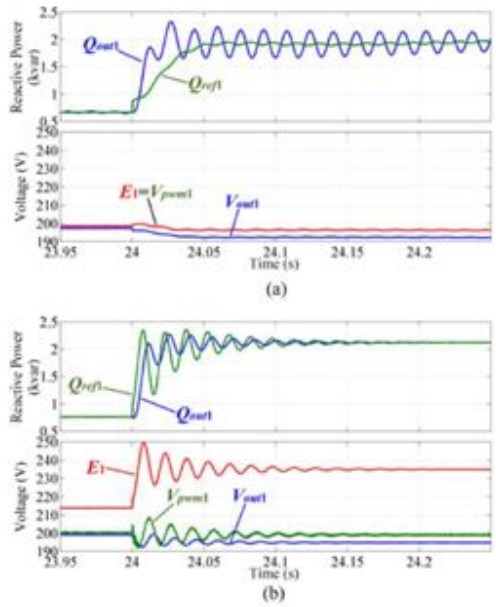

Fig. 11. Zoom-in simulation results of reactive power and voltage of DG1 at 24 s. (a) The basic VSG control; (b) the proposed enhanced VSG control

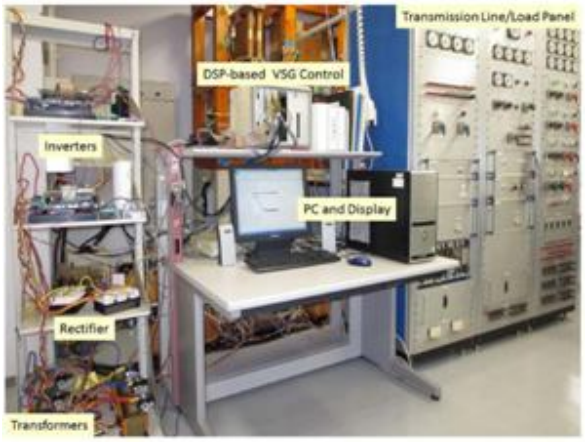

Fig. 12. Setup of experiment system.

TABLE IV
EXPERIMENT SEQUENCE

Time	$P^*_{0\_1}$	$P^*_{0\_2}$	Load
$t < 0.5$ s	1 pu	1 pu	Load1
0.5 s $\leq t <$ 3 s	–	–	Load1+2
3 s $\leq t <$ 5 s	–	0.6 pu	–

VII. EXPERIMENTAL RESULTS

Experiments are executed in an islanding microgrid, of which the circuit is the same as that of simulation shown in Fig. 9, except that instead of dc sources, ac supply rectified by diode bridges is used to imitate the dc output of DGs, and the breaker BK3 is opened. The setup of experiment sys-tem is shown in Fig. 12 and experiment sequence is shown in Table IV. Control Parameters are the same as those listed in Table II, and the experimental results are shown in Fig. 13.

Experimental results verify again the effectiveness of the proposed enhanced VSG control. First, the oscillation due to loading transition at 0.5 s is eliminated, and the oscilla-tion due to change of set value of acitive power at 3.0 s is damped. It implies that the proposed enhanced VSG control

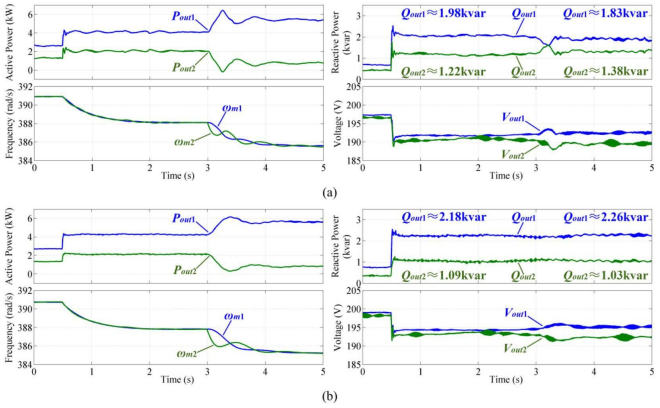

Fig. 13. Experimental results of active power and frequency in the left column and reactive power and voltage in the right column when both DGs are controlled by (a) the basic VSG control, (b) the proposed enhanced VSG control.

is able to track the loading transition rapidly and accu-rately without oscillation; meanwhile, the inertia support of the basic VSG control is kept. Even when an oscillation occurs, the overshoot is suppressed owing to increased system damping.

Furthermore, by applying the enhanced VSG control, reac-tive power is shared according to power rating ratio, and is immune to active power sharing change and line impedance mismatch in per unit values. Although ripples in RMS value of output voltage can be observed due to a slight load unbal-ance, the reactive power is controlled well when the enhanced VSG control is applied.

VIII. CONCLUSION

In this paper, an enhanced VSG control is proposed as a novel communication-less control method in a microgrid. A stator reactance adjuster is developed based on state-space analyses, in order to increase the active power damping and to properly share transient active power. A novel communication-less reactive power control strategy based on inversed voltage droop control (V–Q droop control) and common ac bus voltage estimation is also proposed to achieve accurate reactive power sharing, which is immune to active power sharing change and line impedance mismatch. Simulation and experimental results demonstrated that the

proposed enhanced VSG control achieves desirable transient and steady-state performances, and keeps the inertia support feature of VSG control. As a result, the proposed enhanced VSG control is a preferable choice for the control system of DGs in microgrids.

REFERENCES

[1] R. H. Lasseter, "Microgrids," in *Proc. IEEE Power Eng. Soc. Winter Meeting*, New York, NY, USA, 2002, pp. 305–308. J. M. Guerrero,

[2] J. C. Vasquez, J. Matas, L. G. de Vicuña, and M. Castilla, "Hierarchical control of droop-controlled AC and DC microgrids—general approach toward standardization," *IEEE Trans. Ind. Electron.*, vol. 58, no. 1, pp. 158–172, Jan. 2011.

[3] A. Bidram and A. Davoudi, "Hierarchical structure of microgrids con-trol system," *IEEE Trans. Smart Grid*, vol. 3, no. 4, pp. 1963–1976, Dec. 2012.

[4] M. C. Chandorkar, D. M. Divan, and R. Adapa, "Control of parallel connected inverters in standalone AC supply systems," *IEEE Trans. Ind. Appl.*, vol. 29, no. 1, pp. 136–143, Jan./Feb. 1993.

[5] H. Bevrani, M. Watanabe, and Y. Mitani, *Power System Monitoring and Control.* Hoboken, NJ, USA: Wiley, 2014.

[6] J. M. Guerrero, J. Matas, L. G. De Vicuña, M. Castilla, and J. Miret, "Decentralized control for parallel operation of distributed generation inverters using resistive output impedance," *IEEE Trans. Ind. Electron.*, vol. 54, no. 2, pp. 994–1004, Apr. 2007.

[7] T. L. Vandoorn, B. Meersman, L. Degroote, B. Renders, and Vandevelde, "A control strategy for islanded microgrids with DC-link voltage control," *IEEE Trans. Power Del.*, vol. 26, no. 2, pp. 703–713, Apr. 2011.

[8] T. L. Vandoorn, B. Meersman, J. D. M. De Kooning, and L. Vandevelde, "Analogy between conventional grid control and islanded microgrid con-trol based on a global DC-link voltage droop," *IEEE Trans. Power Del.*, vol. 27, no. 3, pp. 1405–1414, Jul. 2012.

[9] J. C. Vasquez, J. M. Guerrero, M. Savaghebi, J. Eloy-Garcia, and Teodorescu, "Modeling, analysis, and design of stationary-reference-frame droop-controlled parallel three-phase voltage source inverters," *IEEE Trans. Ind. Electron.*, vol. 60, no. 4, pp. 1271–1280, Apr. 2013.